From ferromagnetism to incommensurate magnetic structures: A neutron diffraction study of the chemical substitution effects in $TbPt_{1-x}Cu_x$

A. Señas,[1] J. Rodríguez Fernández,[1] J. C. Gómez Sal,[1] J. Campo,[2] and J. Rodríguez-Carvajal[3]
[1]*DCITIMAC, Facultad de Ciencias, Universidad de Cantabria, Santander 39005, Spain*
[2]*Instituto de Ciencia de Materiales de Aragón, CSIC-Universidad de Zaragoza, Zaragoza 50009, Spain*
[3]*Laboratoire Léon Brillouin, C.E.A.-C.N.R.S., CEA Saclay, 91191 Gif sur Yvette, France*
(Received 4 June 2004; published 19 November 2004)

We report the magnetic structures of the $TbPt_{1-x}Cu_x$ system obtained by means of neutron diffraction experiments. Symmetry analyses have been carried out for the R^{3+} magnetic site. The compounds with copper concentrations $x<0.3$ present the same magnetic structure than the extreme TbPt, which is of noncollinear ferromagnetic type, $-C_xF_z$; on the contrary, for copper concentrations $0.3<x<0.5$, we found incommensurate amplitude-modulated structures in which the moment modulus varies sinusoidally with a propagation vector along the **b**-axis. For concentrations $x>0.5$, the propagation vector lies in the **ac**-plane being the structure also amplitude-modulated. For the intermediate compound, $TbPt_{0.7}Cu_{0.3}$, we observe an evolution from an amplitude-modulated incommensurate structure to a noncollinear commensurate one, $-C_xF_z$, that remains stable down to very low temperatures. The different kinds of magnetic ordering in the $TbPt_{1-x}Cu_x$ series, along which the volume remains constant, are discussed in terms of the competition between RKKY interactions and magneto-crystalline anisotropy, and they are compared to those observed in $TbNi_{1-x}Cu_x$.

DOI: 10.1103/PhysRevB.70.184425 PACS number(s): 75.25.+z, 75.50.Cc, 75.50.Ee

I. INTRODUCTION

The study of substitutional metallic compounds has been a useful way to investigate continuous modifications in the basic magnetic interactions that are at the origin of the macroscopic magnetic properties.[1,2]

In some cases, the substitution of an ion by another with smaller volume, as in $Tb_{1-x}Y_xCu$,[3] mainly induces cell volume effects that can be considered as "chemical pressure effects." In other cases, this substitution may produce modifications on the conduction band, affecting the electric and transport properties and the magnetic ground state of the compounds. The substitution compounds have provided some of the clearest examples of interesting magnetic phenomena, such as:

(a) Single magnetic ground states consisting in the stabilization of modulated structures at low temperatures in non-Kramers ions[4] or the evolution to equal moment structures in the Kramers ones.[5]
(b) The existence of incommensurate magnetic structures associated to complicated two dimension or three dimensional propagation vectors, contributing to a larger complexity in the magnetic arrangements.[6,7]
(c) The finding of non-Fermi liquid states as observed in the $U_{1-x}Y_xPd_3$ (Ref. 8) or $CeCu_{6-x}Au_x$ (Ref. 9) systems.

The main problem with chemical substitutions is the introduction of intrinsic structural disorder in the compounds, which sometimes gives rise to inhomogeneities deriving in phase segregations,[10] cluster glasses[11,12] or spin glass phases.[13] These inhomogeneities can be intrinsic and have been detected in many of the current interesting materials as high T_C superconductors,[14] manganites[15] or strongly correlated electron systems.[16,17]

One common fact appearing in substitutional series is the changes in the magnetic character of the compounds. For example the cubic TbCu antiferromagnetic structure evolves to a ferromagnetic collinear arrangement for a large amount of Zn substitutions in $TbCu_{1-x}Zn_x$;[18] the $GdCu_{1-x}Ga_x$ system presents also a similar evolution;[19] an "anomalous" transition from antiferromagnetism to ferromagnetism has been evidenced in $TbNi_{1-x}Cu_xAl$ (Ref. 20) and $Tb_{1-x}Y_xNiAl$ (Ref. 21) series. In these last series, it was established that both FM and AFM order coexist in different domains of the same sample and the preferred type of order changes with temperature.

The origin of such evolution is still a matter of controversy and combined effects of interionic distances and band structure effects are usually invoked.[22,23] Since in most of the cases both effects, chemical pressure and changes in the conduction band, are correlated, then an important issue would be to investigate in a separate way each one of these effects.

In the course of a general study of pseudobinary R(Ni/Pt)Cu compounds, keeping the same FeB orthorhombic structure, we have found that the FM to AFM change appears always approaching the RCu limit. However, while $RNi_{1-x}Cu_x$ presents an increase of the cell volume of about 4%,[24] in the $RPt_{1-x}Cu_x$ series, the volume remains constant in the whole substitutional range (see Fig. 1). Considering that a Cu atom contributes one additional electron to the conduction band when replacing a Pt atom; by increasing the Cu concentration in the $RPt_{1-x}Cu_x$ family we dispose of a good candidate to analyze, independently of volume effects, pure electronic effects (change of the number of conduction electrons) in their magnetic behavior.

Recently we have published a large report on the preparation, thermal treatments and magnetic properties of the

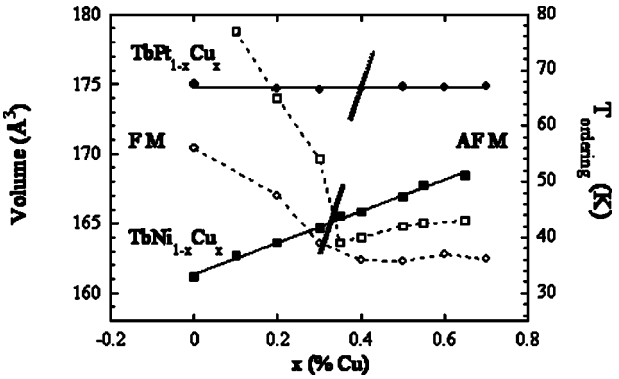

FIG. 1. Cell volume at 300 K and ordering temperatures of the compounds $TbPt_{1-x}Cu_x$ and $TbNi_{1-x}Cu_x$. Vertical marks indicate the region for which the change FM-AFM occurs.

$TbPt_{1-x}Cu_x$ series.[25] After annealing, homogeneous and single crystallographic phases have been obtained, as showed by x ray, neutrons and SEM studies. The change from FM to AFM occurs in the $TbPt_{0.7}Cu_{0.3}$ compound where the AFM structure established at 36.9 K evolves to a ferromagnetic ordering taking place at 23.1 K and it remains stable down to low temperatures. From magnetization and susceptibility measurements, it was deduced that the AFM order should be complex, probably with an incommensurate propagation vector.

In this article, we present a complete study of the magnetic structures of the polycrystalline samples of the $TbPt_{1-x}Cu_x$ family according to a precise symmetry analysis.[26] A comparison with the magnetic studies of the $TbNi_{1-x}Cu_x$ series will be very useful in order to understand the physical reasons underlying the complex magnetic behavior of these materials. The neutron diffraction technique turns out to be an indispensable tool to study the balance between the anisotropy effects and the exchange interaction, thus contributing to enlighten some of the tasks described above.

II. CRYSTALLOGRAPHY AND PREVIOUS MAGNETIC CHARACTERIZATION

Polycrystalline samples of $TbPt_{1-x}Cu_x$ compounds with $x=0$, 0.1, 0.2, 0.3, 0.4, and 0.6 were prepared in an arc-furnace under Ar atmosphere and then subjected to thermal treatments at 750 °C, as it is reported elsewhere.[25] X-ray diffraction and SEM analysis determined that all of them were single-phase.

For the neutron diffraction experiments, we crushed the samples into fine powder; in order to release the stress, the powder was sealed in an evacuated quartz ampoule and subsequently annealed again at 750 °C for 2 days.

Neutron diffraction experiments were performed both on G4.1 (Laboratoire Lèon Brillouin, France) and D1B (Institut Laue-Langevin, France) using wavelengths of 2.427 Å and 2.524 Å, respectively. Both diffractometers span an angular range of 80° (2θ mainly from 2° to 82°), having position sensitive detectors of 800 and 400 channels, respectively. Diffraction patterns were collected every 2 K from 1.5 to 60 K, and the analysis was performed by the Rietveld refinement method, using the program FULLPROF.[27] In order to solve the magnetic structures, symmetry analyses have been performed by using the program BASIREPS.[27]

The crystalline structures of the compounds $TbPt_{1-x}Cu_x$ were determined by x-ray diffraction (300 K) and it was described in detail in (Ref. 25). All the compounds studied crystallize in the FeB orthorhombic structure (*Pnma* space group). The Tb^{3+} ions lie in 4*c* sites and the Cu/Pt atoms are randomly distributed in other 4*c* site: $(x, \frac{1}{4}, z)$, $(-x, \frac{3}{4}, -z)$, $(\frac{1}{2}-x, \frac{3}{4}, \frac{1}{2}+z)$, and $(\frac{1}{2}+x, \frac{1}{4}, \frac{1}{2}-z)$, with different values of *x* and *z* parameters. These parameters were refined by the Rietveld least-squares method using the program FULLPROF. It is worth mentioning that the cell volume remains nearly constant ($\Delta V < 0.1\%$) with the Pt/Cu substitutions, which leads to insignificant modifications of the nearest neighbors' distances along the series.

Later analysis at 60 K (paramagnetic state) and 1.5 K from neutron diffraction data obtained at the instrument D1B (ILL, France) with $\lambda = 2.52$ Å, confirmed the stability of the *Pnma* orthorhombic type structure at these low temperatures. The refined parameters at 60 K are reported in Table I. These estimated lattice parameters are slightly smaller than those obtained at 300 K by means of x-ray diffraction, although as it occurs at 300 K the volume remains mostly constant with the Pt/Cu substitution. As it can be observed in Table I, this invariance is due to the small increase in parameter *a*, while parameters *b* and *c* decrease. The temperature dependence of the cell volume along the series is displayed in Fig. 2, in

TABLE I. Cell parameters and atomic positions in the crystallographic cell refined from the neutron diffraction diagrams at 60 K for the annealed compounds of $TbPt_{1-x}Cu_x$.

					At. Pos. Tb^{3+}		At. Pos. Pt/Cu		
x	*a* (Å)	*b* (Å)	*c* (Å)	*V* (Å^3)	*x*	*z*	*x*	*z*	R_{Bragg}
0.2	7.0024(3)	4.4823(2)	5.5293(2)	173.55	0.182(1)	0.137(2)	0.038(1)	0.650(2)	6.3%
0.3	7.0204(6)	4.4789(4)	5.5255(5)	173.74	0.179(1)	0.145(1)	0.038(1)	0.647(2)	6.8%
0.4	7.0387(4)	4.4675(4)	5.5135(3)	173.37	0.168(1)	0.149(2)	0.035(1)	0.641(2)	8.2%
0.5	7.0735(4)	4.4598(3)	5.5002(3)	173.51	0.185(1)	0.151(1)	0.033(1)	0.653(1)	7.2%
0.6	7.0825(4)	4.4597(3)	5.4853(3)	173.26	0.177(1)	0.145(1)	0.031(1)	0.631(2)	6.5%
0.7	7.0990(2)	4.4587(9)	5.4796(1)	173.44	0.179(1)	0.135(1)	0.036(1)	0.640(2)	6.1%

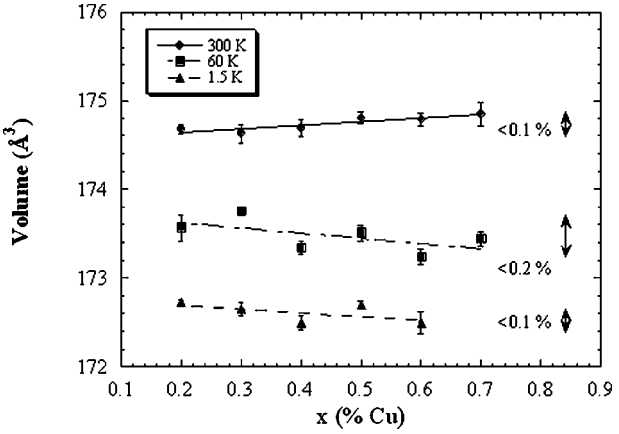

FIG. 2. Cell volume of the annealed $TbPt_{1-x}Cu_x$ compounds at 300 (x ray), 60 and 1.5 K.

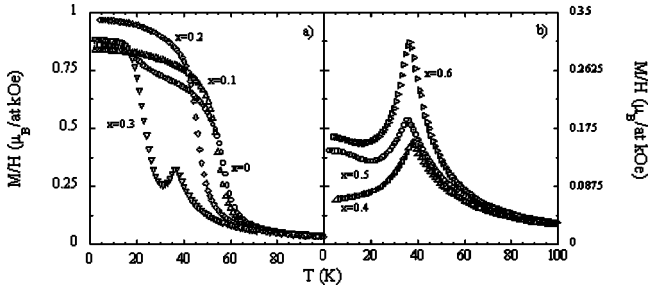

FIG. 3. Thermal variation of the magnetization of the annealed $TbPt_{1-x}Cu_x$ compounds under a constant magnetic field of 2 kOe. Notice the different scale of both graphics.

which we present the results obtained at 300 K (x rays), 60 and 1.5 K (neutron diffraction). The relative volume variation between 300 and 1.5 K, $\Delta V/V$, was estimated to be 6×10^{-3}, very similar to the values obtained for other rare earth intermetallics.[28]

The magnetic characterization of the series has been recently reported,[25] and it is summarized in Fig. 3, where it is presented the magnetic susceptibility M/H versus temperature curves of the diluted compounds under a constant applied magnetic field of 2 kOe. This figure illustrates the existence of two different magnetic behaviors: the compounds with copper concentration $x \leqslant 0.2$ show a clear ferromagnetic character, while those with $x > 0.3$ present an antiferromagnetic behavior. The limit compound ($x=0.3$) shows an antiferromagnetic peak in its susceptibility and, at a lower temperature, it displays a ferromagnetic signal. This fact is due to a phase transition from one to the other kind of magnetic behavior induced by lowering the temperature. The details of this magnetic phase transition will be examined along the next section.

III. MAGNETIC STRUCTURES

A. Ferromagnetic $TbPt_{1-x}Cu_x$ compounds ($x < 0.3$)

Upon cooling, a transition from the paramagnetic to an ordered state is clearly detected in the neutron diffraction patterns. Below a certain temperature (47 K for $TbPt_{0.8}Cu_{0.2}$ and 56 K for TbPt), due to the magnetic ordering, some additional diffraction peaks, which are forbidden by the symmetry rules of the *Pnma* structure, are observed in the neutron patterns simultaneously with an increase of the intensity of the nuclear reflections. All the magnetic peaks can be indexed with integral numbers in the primitive orthorhombic cell so that the propagation vector is $\mathbf{k}=(0,0,0)$ and the group of the propagation vector coincides with the full space group *Pnma*. As commented above, the Tb^{3+} magnetic ions in the crystallographic lattice lie in 4*c* sites. For this Wyckoff position, the eight one-dimensional irreducible representations of the propagation vector space group ($G_{\mathbf{k}}=Pnma$) are given in Table II, together with the corresponding basis functions. The numbering of magnetic atoms (sublattices) of the 4*c* site in a primitive cell are given in the following order $1:(x,\frac{1}{4},z)$, $2:(1-x,\frac{3}{4},1-z)$, $3:(\frac{1}{2}-x,\frac{3}{4},\frac{1}{2}+z)$, and $4:(\frac{1}{2}+x,\frac{1}{4},\frac{1}{2}-z)$. For the basis functions we use the symbols A(+−−+), C(++−−), G(+−+−), and F(++++) corre-

TABLE II. Irreducible representations of the propagation vector group for $\mathbf{k}=(0,0,0)$ in *Pnma* ($G_{\mathbf{k}}=Pnma$) and basis functions for axial vectors bound to the Wyckoff site *4c* ordered in the following way: $1(x,\frac{1}{4},z)$, $2(1-x,\frac{3}{4},1-z)$, $3(\frac{1}{2}-x,\frac{3}{4},\frac{1}{2}+z)$, and $4(\frac{1}{2}+x,\frac{1}{4},\frac{1}{2}-z)$. The global magnetic representation Γ_m decomposes as: $\Gamma_m=\Gamma_1\oplus 2\Gamma_2\oplus 2\Gamma_3\oplus\Gamma_4\oplus\Gamma_5\oplus 2\Gamma_6\oplus 2\Gamma_7\oplus\Gamma_8$, so the total number of basis function for each representation is either one or two.

	1	2_{1z}	2_{1y}	2_{1x}	−1	*a*	*m*	*n*	Basis functions for site *4c*
Γ_1	1	1	1	1	1	1	1	1	$(0,C_y,0)$
Γ_2	1	1	1	1	−1	−1	−1	−1	$(A_x,0,G_z)$
Γ_3	1	1	−1	−1	1	1	−1	−1	$(C_x,0,F_z)$
Γ_4	1	1	−1	−1	−1	−1	1	1	$(0,A_y,0)$
Γ_5	1	−1	1	−1	1	−1	1	−1	$(0,F_y,0)$
Γ_6	1	−1	1	−1	−1	1	−1	1	$(G_x,0,A_z)$
Γ_7	1	−1	−1	1	1	−1	−1	1	$(F_x,0,C_z)$
Γ_8	1	−1	−1	1	−1	1	1	−1	$(0,G_y,0)$

TABLE III. Magnetic structures of the annealed compounds of the series $TbPt_{1-x}Cu_x$ obtained at 1.5 K, given in spherical coordinates: θ is the angle with the *x*-axis and φ is the angle with the *z*-axis; ϕ is the phase due to the modulation in the atoms $2:(-x,-\frac{1}{4},-z)$ and $3:(\frac{1}{2}-x,-\frac{1}{4},\frac{1}{2}+z)$.

x (Cu)	*T* (K)	Structure	*k*	Type	μ (μ_B)	θ	φ	ϕ	R_B (%)
0	56	FM non-collinear	(0 0 0)	−C*x*Fz	8.3	180°	39°	0	7
0.2	≤47.6	FM non-collinear	(0 0 0)	−C*x*Fz	8.6	180°	50.2°	0	3.2
0.3	≤30	FM non-collinear	(0 0 0)	−C*x*Fz	7.28	180°	47.8°	0	5.5
	21–39	AM	(0 0.17 0)	C*x*G*y*Fz	5.18	167°	145°	30.8°	5.4
0.4	≤36	AM	(0 0.23 0)	C*x*G*y*Fz	9	6.1°	136°	41.6°	3
0.5		?	$\lvert\mathbf{k}\rvert=0.29$						
0.6	≤37	AM	(0.15 0 0.23)	(*xyz*)	7.6	0°	102°	90°	10
0.7		?	$\lvert\mathbf{k}\rvert=0.25$						

sponding to the well known Bertaut's notations.[29] Finally, the representations Γ_1, Γ_4, Γ_5, and Γ_8 are associated with collinear magnetic structures along the *y*-axis, while Γ_2, Γ_3, Γ_6, and Γ_7 correspond to noncollinear orderings within the plane (*x z*), which is the mirror plane associated to the 4*c* site.

The best agreement between the calculated and the observed neutron diffraction pattern (below T_C) is obtained for the magnetic structure described by the representation Γ_3. The refined structure corresponds to a noncollinear model $-C_xF_z$, in which all the magnetic ions in the unit cell present ferromagnetic ordering along the *z*-axis, the moments having antiferromagnetic components along the *x*-axis. At 1.5 K, the refined values of the magnetic moments oscillate around 8.25 μ_B, slightly reduced below the expected value of the free ion of Tb^{3+} of $\mu=g_JJ\mu_B=9$ μ_B. This small reduction is quite common in the intermetallic rare-earth compounds, as for example in $TbNi_2$ ($\mu=8.3$ μ_B),[30] and is certainly due to the crystal electric field effects. The angle with the *z*-axis increases with the Cu content, thus, the antiferromagnetic component increases along the series. All the refined values of free parameters are given in Table III. As an example, the plot corresponding to the refinement of the patterns recorded at 60 and 1.5 K for $TbPt_{0.8}Cu_{0.2}$ is shown in Fig. 4.

In Fig. 5, we show a scheme of the magnetic structure of the family $TbPt_{1-x}Cu_x$ for $x<0.3$. The magnetic ordering coincides with the magnetic structure determined by Castets *et al.*[31] for the binary TbPt compound.

B. The intermediate compound $TbPt_{0.7}Cu_{0.3}$

In Fig. 6, we present the thermodiffractogram of the compound $TbPt_{0.7}Cu_{0.3}$ measured at D1B between 60 and 1.5 K in steps of 2 K. Below 39 K, the neutron diffraction patterns contain many additional reflections relative to those observed in the paramagnetic regime. The low-angle intense peak and other additional reflections can be indexed with a propagation vector $\mathbf{k}=(0,\delta,0)$, $\delta\approx0.17$, corresponding to an incommensurate magnetic structure. This set of peaks progressively disappears when the temperature is lowered whereas a second set of reflections, indexed with $\mathbf{k}=(0,0,0)$, emerges. Below 20 K only the reflections of the second set, which are similar to those appearing in the ferromagnetic compounds, are observed.

In Fig. 7 we show the thermal dependence of the integrated magnetic peak intensity of the $(0\ 0\ 0)\pm\mathbf{k}=(0\ \pm\delta\ 0)$ reflection, together with the commensurate (0 0 1) one. From the figure one can see that the ordering temperatures correspond to $T_N=39$ K and $T_C=30$ K, respectively. The solid lines are guides to the eyes, and the intensities have been normalized. It can be observed that both structures coexist in the temperature range $30>T>21$ K.

In order to determine the magnetic structure of the Tb^{3+} spins in the site 4*c* of the *Pnma* unit cell in the incommensurate region with $\mathbf{k}=(0,\delta,0)$, a symmetry analysis has been performed using the program BASIREPS.[27] It provides four one-dimensional irreducible representations. The complete set of results, representations plus basis functions are gathered in Table IV. In this case, the best refinement corresponds strictly to the representation $\Gamma_3^{\mathbf{k}}$. The least-squares

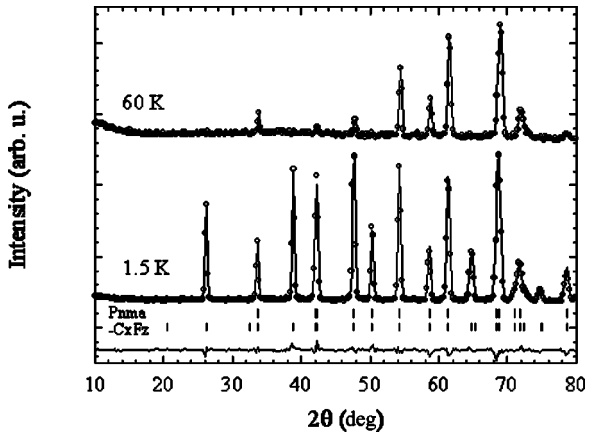

FIG. 4. Neutron diffraction diagrams of the compound $TbPt_{0.8}Cu_{0.2}$ at 60 and 1.5 K. The vertical marks correspond to the Bragg positions for the phase indicated in the figure.

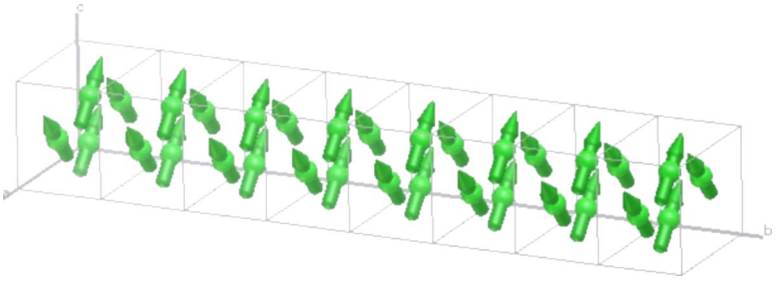

FIG. 5. (Color online) Magnetic structure of $TbPt_{1-x}Cu_x$ with $x<0.3$ of type $-CxFz$.

Rietveld analysis using the FULLPROF program revealed that the Tb^{3+} ions order as a longitudinal sinusoidally modulated structure along the *y*-axis with the magnetic moments arranged like (C_x, G_y, F_z). This is the same mode as the commensurate structure within the *xz*-plane. The amplitude of the magnetic moments at 33 K is 5.18 μ_B. This and other derived parameters are all listed in Table III. In Fig. 8, we show the magnetic incommensurate structure refined for this compound at high temperatures, the sine wave represented by a solid line.

Below 30 K, the magnetic structure of $TbPt_{0.7}Cu_{0.3}$ is ferromagnetic noncollinear, of $(-C_x, 0, F_z)$ type, similar to that described above for the compounds with lower Cu content. At 1.5 K, the refined value for the magnetic moment of Tb^{3+} is 7.28 μ_B, which is smaller than the value determined for the previous ferromagnetic compounds (8.25 μ_B). The angle with the *z*-axis is 132.5°, thus the ferromagnetic component decreasing with *x* just as it happened with the compounds $x<0.3$. In Table III, we have reported all the refined parameters corresponding to this commensurate structure. In this region, we have observed an anisotropic strain broadening of those peaks with indexes $(h\ k\ l)$, $k\neq 0$. This phenomenon along the *y*-axis could be owed to some reminiscence of the high-temperature incommensurate structure that varies sinusoidally along that direction. The situation can then be described like if there were defects in the structure so that magnetic moment inversions, $(C_x, 0, -F_z)$, or other more complicated kind of defects occur mostly along the [010] direction. The averaged maximum strain, deduced from the additional integral breadth of the $k\neq 0$ reflections, is 86.3 $\times 10^{-4}$ with an anisotropy of 47.6×10^{-4}. Along the direction [010] the strain value is 158.7×10^{-4} and the reflections $(h0l)$ have no strain. Thus, the unusual huge reduction of the magnetic moment is no longer due uniquely to the crystal electric field and could also be associated with such reminiscence phenomenon. Similarly, an important reduction of the magnetic moment of Tb was found in the antiferromagnetic $TbMn_2D_2$ ($\mu=4.8\ \mu_B$), although in this case it was attributed to a diffuse scattering due to the partial disorder of the Tb moments.[32]

C. The antiferromagnetic compound $TbPt_{0.6}Cu_{0.4}$

The main feature for the neutron diffraction diagrams of $TbPt_{0.6}Cu_{0.4}$ below $T_N=36$ K is the existence of a huge magnetic peak at 7° associated to a few weak reflections at higher angles, which can be indexed with a propagation vector $\mathbf{k}=(0, 0.23, 0)$, nearly equal to the one observed in $TbPt_{0.7}Cu_{0.3}$ at high temperature. However, in contrast to this last case, in the $TbPt_{0.6}Cu_{0.4}$ compound the same pattern is observed in the whole temperature range.

In Fig. 9, we show the powder diffraction diagram of $TbPt_{0.6}Cu_{0.4}$ at 1.5 K along with its refinement by means of least-square method. The symmetry analysis performed for the $x=0.3$ compound in its incommensurate phase is also valid for this case (see Table IV). In this case, the best agreement between the model and the experimental magnetic intensities is obtained also for the single representation $\Gamma_3^{\mathbf{k}}$,

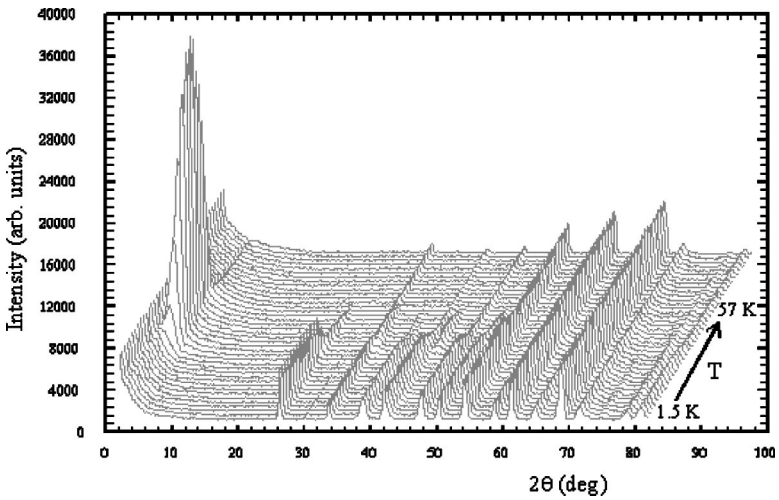

FIG. 6. Thermodiffractogram of the compound $TbPt_{0.7}Cu_{0.3}$ for temperatures between 1.5 and 60 K.

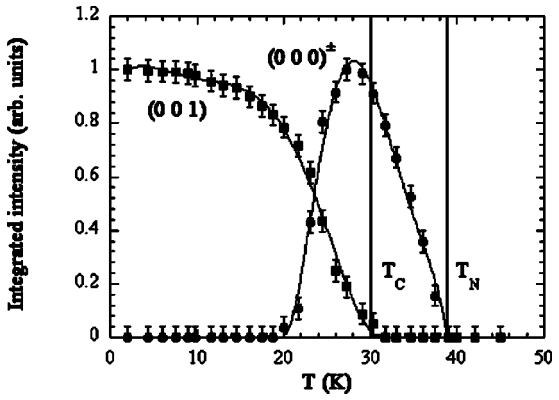

FIG. 7. Thermal dependence of the $(0\ 0\ 0)^{\pm}$ and $(0\ 0\ 1)$ reflections corresponding to the incommensurate and ferromagnetic noncollinear $-CxFz$ structures, respectively, of the compound $TbPt_{0.7}Cu_{0.3}$. The vertical lines correspond to the ordering temperatures of each magnetic phase.

corresponding to a mode (C_x, G_y, F_z). The maximum value ofthe ordered magnetic moment at the lowest temperature is 9 μ_B, very close to the expected value for the free ion.

D. The antiferromagnetic compound $TbPt_{0.4}Cu_{0.6}$

Below 37 K, the neutron diffraction diagrams of $TbPt_{0.4}Cu_{0.6}$ contain a new set of reflections of magnetic origin characterized by a strong line at low angles, which are incommensurate with the nuclear cell. The propagation vector that indexes these new peaks is $\mathbf{k}=(0.15,0,0.23)$, being the unique magnetic transition in the whole temperature range. In this case, from mere symmetry considerations on the *Pnma* structure with a propagation vector in the plane (x,z), the relative values and orientations of the magnetic moments are no longer predetermined. All Tb atoms become independent from the symmetry point of view, except that for each Tb atom the components of the magnetic moments should be either perpendicular or within the plane (x,z). An appealing result in terms of Monte Carlo analysis at 1.5 K is that the refinements improve considerably when we restrict the maximum value of the moments to be equal, with a value of 7.6 μ_B, and the structure is amplitude modulated, all the calculated parameters being reported in Table III. We have refined the magnetic structure constraining all moment amplitudes to be the same and the vectors within the (x,z) plane. The refinement of the experimental pattern at 1.5 K in terms of this tentative structure is displayed in Fig. 10.

E. The antiferromagnetic compounds $TbPt_{0.5}Cu_{0.5}$ and $TbPt_{0.3}Cu_{0.7}$

The antiferromagnetic compounds $TbPt_{0.5}Cu_{0.5}$ and $TbPt_{0.3}Cu_{0.7}$ have been also analyzed by means of neutron diffraction. Unfortunately, the homogenization thermal process in these cases was not totally completed,[25] thus providing the diagrams several magnetic contributions due to phase segregation. Nevertheless, the signal at low angles is very clear and should be owed to a unique antiferromagnetic incommensurate structure for which the modulus of its propagation vector, $|\mathbf{k}|$ can be calculated, as shown in Table III.

F. The ferromagnetic $TbNi_{0.7}Cu_{0.3}$ and antiferromagnetic $TbNi_{0.6}Cu_{0.4}$ compounds

Two compositions of the isomorphous $TbNi_{1-x}Cu_x$ series have been selected in order to precisely determine their magnetic structures as a comparison to the Pt-based ones; in particular, we have synthesized $TbNi_{0.7}Cu_{0.3}$ and $TbNi_{0.6}Cu_{0.4}$ samples, ferro- and antiferromagnetic, respectively. The analysis of the diffraction diagrams using the Rietveld method and the group theory for both commensurate and

TABLE IV. Irreducible representations of the propagation vector group for $\mathbf{k}=(0,\delta,0)$ in *Pnma* ($G_k = Pn2_1a$) and basis functions for axial vectors bound to the Wyckoff site *4c* ordered in the following way: $1(x,\frac{1}{4},z)$, $2(1-x,\frac{3}{4},1-z)$, $3(\frac{1}{2}-x,\frac{3}{4},\frac{1}{2}+z)$, and $4(\frac{1}{2}+x,\frac{1}{4},\frac{1}{2}-z)$. All representations are one-dimensional. The global magnetic representation Γ_m decomposes as: $\Gamma_m = 3\Gamma_1^k \oplus 3\Gamma_2^k \oplus 3\Gamma_3^k \oplus 3\Gamma_4^k$, so the total number of basis function for each representation is three. We have used the notation $\alpha = \exp(i\pi\delta)$ and $\xi = \alpha^* = \exp(-i\pi\delta)$.

					Basis functions for site *4c*				
	1	2_{1y}	a	n	Tb1	Tb2	Tb3	Tb4	Bertaut notation
Γ_1^k	1	α	1	α	(1, 0, 0)	$(-\xi, 0, 0)$	$(\xi, 0, 0)$	(−1, 0, 0)	G_x
					(0, 1, 0)	$(0, \xi, 0)$	$(0, -\xi, 0)$	(0, −1, 0)	C_y
					(0, 0, 1)	$(0, 0, -\xi)$	$(0, 0, -\xi)$	(0, 0, 1)	A_z
Γ_2^k	1	α	−1	$-\alpha$	(1, 0, 0)	$(-\xi, 0, 0)$	$(-\xi, 0, 0)$	(1, 0, 0)	A_x
					(0, 1, 0)	$(0, \xi, 0)$	$(0, \xi, 0)$	(0, 1, 0)	F_y
					(0, 0, 1)	$(0, 0, -\xi)$	$(0, 0, \xi)$	(0, 0, −1)	G_z
Γ_3^k	1	$-\alpha$	1	$-\alpha$	(1, 0, 0)	$(\xi, 0, 0)$	$(-\xi, 0, 0)$	(−1, 0, 0)	C_x
					(0, 1, 0)	$(0, -\xi, 0)$	$(0, \xi, 0)$	(0, −1, 0)	G_y
					(0, 0, 1)	$(0, 0, \xi)$	$(0, 0, \xi)$	(0, 0, 1)	F_z
Γ_4^k	1	$-\alpha$	−1	α	(1, 0, 0)	$(\xi, 0, 0)$	$(\xi, 0, 0)$	(1, 0, 0)	F_x
					(0, 1, 0)	$(0, -\xi, 0)$	$(0, -\xi, 0)$	(0, 1, 0)	A_y
					(0, 0, 1)	$(0, 0, \xi)$	$(0, 0, -\xi)$	(0, 0, −1)	C_z

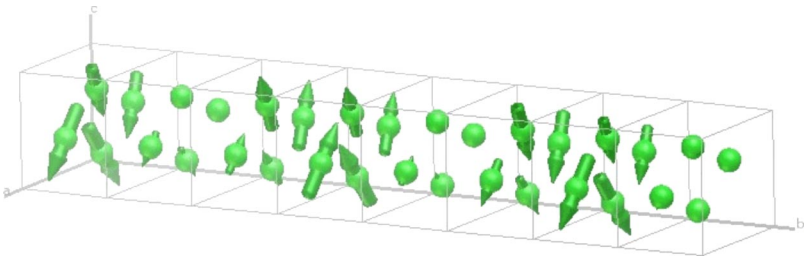

FIG. 8. (Color online) Incommensurate magnetic structure of the annealed $TbPt_{0.7}Cu_{0.3}$ compound at 33 K.

incommensurate structures has reproduced with good fidelity previous results obtained from the analysis of the integrated intensities,[24] although some slight modifications in the incommensurate structure for $x=0.4$ were found.

For $TbNi_{0.7}Cu_{0.3}$, the statements described for TbPt in Sec. III A are still valid and thus we can assume the eight one-dimensional irreducible representations of the *Pnma* space group and $\mathbf{k}=(0,0,0)$ given in Table II. In this case, among all the allowed modes, the best agreement between the calculated and the observed neutron diffraction patterns (below T_C) is obtained for the representation Γ_7, providing a noncollinear structure F_xC_z for which all the magnetic moments are aligned ferromagnetically along the *x*-axis and antiferromagnetically along *z*. At 1.5 K, the refined value of the magnetic moment is 8.3 μ_B, similar to those found in the Pt-based series, and the angle with the *x*-axis is −33°. The refined values are all listed in Table III.

Below the Néel temperature, $T_N=39.4$ K, the antiferromagnetic $TbNi_{0.6}Cu_{0.4}$ compound presents a set of new reflections characterized by a huge peak at low angles that can be indexed with a propagation vector $\mathbf{k}=(0,0.15,0)$ and remains stable down to 1.5 K. Symmetry analysis in terms of the group theory for a propagation vector $\mathbf{k}=\mathbf{k}_y$ is reported in Table IV. In this case, the best agreement between the calculated and the experimental magnetic intensities is obtained for representation Γ_7 providing F_xC_z orderings, as for the previous ferromagnetic compound. The maximum value of the modulated magnetic moment at the lowest temperature is 7.4 μ_B and the angle with the *x*-axis is −51°.

Differences found respect to the structures described in Ref. 24 slightly affect the values of the ordering temperatures and the angles with the *x*-axis, which in this case favor the antiferromagnetic component of the moments. All of them can be interpreted as mere details and could be owed to little stoichiometric differences, which are within the experimental error.

IV. DISCUSSION

The refined magnetic structures of the $TbPt_{1-x}Cu_x$ orthorhombic *Pnma* compounds agree with the evolution of their macroscopic magnetic properties.[25] The increment of Cu content in the samples gives rise to complex magnetic structures, which have been determined by symmetry analysis. Regarding the usefulness of the group theory for structure calculations, for our substitutional compounds symmetries are not perfectly well established and so the magnetic orderings correspond to mixtures of irreducible representations, which complicate the magnetic structure determination. For the greater Cu contents, the determination of the magnetic structures is especially difficult, since for the propagation vectors found the group theory does not impose restrictions in the disposition of the moments.

Ferromagnetic noncollinear structures are very common in orthorhombic pseudobinary compounds as a result of the competition between the exchange RKKY interactions and the strong magnetocrystalline anisotropy. In these structures, the anisotropy divides the rare earth ions into two sublattices with different magnetization directions in the (x,z) plane. The structures determined in the present case, which are of $-C_xF_z$ type, coincide with that previously found in TbPt.[31]

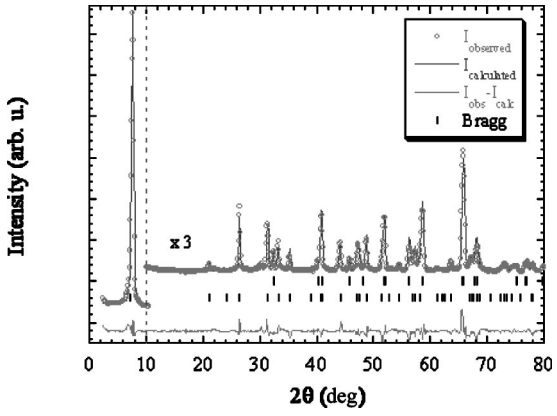

FIG. 9. Neutron diffraction diagram of the compound $TbPt_{0.6}Cu_{0.4}$ at 1.5 K. The two sets of vertical marks correspond to the Bragg positions for the nuclear and incommensurate phases, respectively. The scale in the region 10°–80° has been incremented in a factor 3.

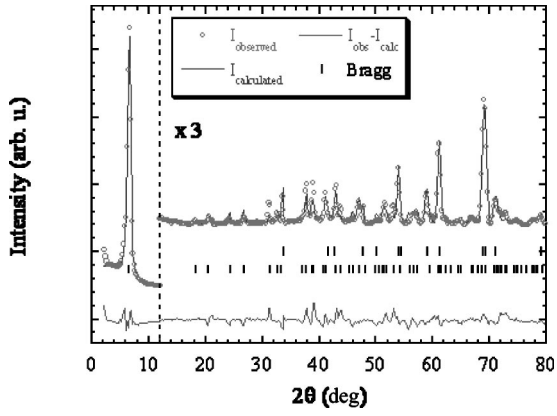

FIG. 10. Neutron diffraction diagram of the compound $TbPt_{0.4}Cu_{0.6}$ at 1.5 K. The two sets of vertical marks correspond to the Bragg positions for the nuclear and incommensurate phases, respectively. The scale in the region 12°–80° has been incremented in a factor 3.

However, the magnetic structures of $TbPt_{1-x}Cu_x$ compounds are different from those of $TbNi_{1-x}Cu_x$,[24] since the directions of the ferromagnetic components are not the same: it is along *z*-axis in the Pt-compounds and along *x*-axis in the Ni-ones. Castets *et al.*[31] propose that these differences are based in the variation of the surroundings of the ion owed to the bigger atomic volume of Pt; consequently, the quadrupole of the neighboring atoms is modified. Due to this fact, the V_2^{-2}/V_2^2 ratio between second-order parameters of the crystal field, which provides the quadrupole directions of the vicinity, are on either side of the $-\pi/2$ value, and so, the direction of the ferromagnetic components must be different for RNi and RPt compounds. In particular, they established that for Tb^{3+} ions, in which $\alpha_J<0$ (α_J is the ionic quadrupole, acting on the dominant second-order term of the crystal field Hamiltonian), the direction of the ferromagnetic component is parallel to a in RNi compounds and parallel to **c** in RPt compounds, which coincides exactly with our results.

The progressive increase of the number of conduction electrons contributed by Cu favors the negative exchange interactions and the structures become complex: the Fourier transform of the exchange integral, which is dependent of the polarization of conduction electrons, becomes maximal for $\mathbf{k}\neq 0$ and so the magnetic periodicity is now incommensurate with the nuclear unit cell. Incommmensurate magnetic phases are widely observed in rare earth intermetallics: they occur as a result of competing long range interactions between the localized $4f$ moments via the polarization of the conduction band and the influence of the crystalline field induced anisotropy and small quadrupole-quadrupole interactions.[33] The exchange interactions in rare earth intermetallic compounds are indirect and of RKKY type, mediated by the polarization of the conduction electrons, the radial extent of the rare earth $4f$ shells being too small for direct interactions. Due to the low symmetry of rare earth site it is likely that crystal field effects become of importance and may introduce an important anisotropy and strongly fix the moment direction.

In the present series, the appearance of modulated structures for concentrations $x\geqslant 0.3$ confirms the existence of a strong anisotropy in these $TbPt_{1-x}Cu_x$ compounds: the magnetocrystalline anisotropy imposes the orientation of the magnetic moments, although their amplitudes are sinusoidally modulated along the **k** directions. In this sense, the moment directions in the series mainly remain in the (x,z) plane, although an additional component along the *y*-axis becomes appreciable. In the isomorphous $GdNi_{0.4}Cu_{0.6}$, with negligible magnetocrystalline anisotropy ($L=0$), the incommensurate structure is helimagnetic, $\mathbf{k}=(0,0,0.25)$, and the moments are able to rotate in the (x,y) plane when we move along the *z*-axis.[34]

In addition, all the incommensurate structures in the $TbPt_{1-x}Cu_x$ and $TbNi_{1-x}Cu_x$ series stabilize until very low temperatures, which is only possible due to the non-Kramers character of the Tb^{3+} ion:[35] the R ion in low symmetry sites could have a single ground state; thus, in order to induce a magnetic moment on a non-Kramers ion, the field acting on it has to mix the two first low lying singlet levels. In such a case, the magnetic moments can have any value below $\mu_B g_J J$ without increasing the entropy of the system, so that when the evolution of the conduction band by Cu introduction favors a modulated structure, it can remain stable down to 0 K.

It is clear from the present results that the value of the propagation vector **k** is highly dependent on the composition in the antiferromagnetic compounds. This means that the Fourier transform of the magnetic interactions, $J(\mathbf{k})$, could reach its minimum for different values of **k** out of the symmetry points in the *k*-space. Modifications in the morphology of the Fermi surface, very sensitive to electronic changes, are certainly related to the existence of different **k** values. This situation is reminiscent of the nesting effect,[36] sometimes invoked as the cause of the existence of complex magnetic structures. An important issue revealed from this biunivocal relation between the propagation vector and composition, was useful to determine the coexistence of different phases in the "as quenched" preparations of the series.[37]

The behavior of the intermediate compound $TbPt_{0.7}Cu_{0.3}$ is extremely interesting in which we observe an evolution from an incommensurate amplitude-modulated structure, immediately below the ordering temperature, to a ferromagnetic noncollinear one that remains stable down to low temperatures. It is difficult to ascertain the origin of this behavior. However, in this limit compound, slight modifications in the cell volume when decreasing the temperature, could increase the $n(E_F)$, inducing a ferromagnetic behavior. In addition, crystal electric field modifications with temperature could not be discarded and could give rise to a mix of the two first low lying singlet levels in all the Tb^{3+} ions, thus R ions behaving as effective Kramers ions, as could occur in the higher Pt content compounds.

From the presented results, we can confirm that the AF behavior with complex incommensurated structures is favored by the increasing Cu content, as in other similar series (NiCu, etc.). However, in these cases, this evolution might not be attributed to changes in the interatomic distances. This study clearly demonstrate that the main parameter driving this change is related to electronic effects: (a) modification in the Fermi surface (biunivocal relation between propagation vector and composition), (b) modifications of the density of states in the Fermi level $n(E_F)$; a large value of this number favors a ferromagnetic behavior, as seems to be the case in the intermediate compounds at low temperatures, confirming the suggestions of Ref. 23, where the role of $n(E_F)$ is discussed as well as band calculations on Cu based systems.[38]

V. CONCLUSIONS

In the $TbPt_{1-x}Cu_x$ compounds, the *Pnma* orthorhombic structure remains stable for $x\leqslant 0.7$, with negligible modifications of the interionic distances. For $x<0.3$, the magnetic structures are ferromagnetic noncollinear, of $-CxFz$ type. For $x>0.4$, the magnetic structures are antiferromagnetic incommensurate, with a modulated moment amplitude. In the intermediate $TbPt_{0.7}Cu_{0.3}$ compound, the balance between FM and AFM interactions is critical, and the incommensurate structure evolves towards the ferromagnetic one by decreasing the temperature. Symmetry analysis has been needed to determine these complex magnetic structures, which emerge due to the competition of the RKKY interaction and the strong magnetocrystalline anisotropy.

Finally, band structure modifications associated to the supplementary electrons contributed by Cu ions should be responsible for the changes mainly in the RKKY interactions, which give rise to the appearance of antiferromagnetism with complex magnetic structures without the mediation of distance changes between magnetic ions.

ACKNOWLEDGMENTS

This work was supported by the Spanish CICYT Grant No. MAT2002-04178-c04. The Spanish part of the CRG-D1B is acknowledged for the allocation of beam time in D1B instrument.

[1] H.R. Kirchmayr and C.A. Poldy, *Handbook on the Physics and Chemistry of Rare Earths*, edited by K.A. Gschneidner, Jr. and L. Eyring (North-Holland, Amsterdam, 1979), Vol. 2, p. 55.
[2] J.J.M. Franse and R.J. Radwanski, *Handbook of Magnetic Materials*, edited by K.H.J. Buschow (North-Holland, Amsterdam, 1993), Vol. 7, p. 307.
[3] C.S. Garde and J. Ray, J. Phys.: Condens. Matter **6**, L589 (1994).
[4] D. Gignoux, R. Lemaire, and D. Paccard, Phys. Lett. **A41**, 187 (1972).
[5] D. Gignoux and J.C. Gómez Sal, Phys. Lett. **A50**, 63 (1974).
[6] D. Gignoux and D. Schmitt, Phys. Rev. B **48**, 12682 (1993).
[7] A. Szytula, *Handbook of Magnetic Materials*, edited by K.H.J. Buschow (Elsevier, New York, 1991), Vol. 6, Chap. 2, p. 85.
[8] M.B. Maple, M.C. de Andrade, J. Herrmann, Y. Dalichaouch, D.A. Gajewski, C.L. Scaman, R. Chau, R. Movshovich, M.C. Aronson, and R. Osborn, J. Low Temp. Phys. **99**, 223 (1995).
[9] H. v. Löhneysen, T. Pietrus, G. Portish, H.G. Schlager, A. Schroder, M. Sieck, and T. Trappman, Phys. Rev. Lett. **72**, 3262 (1994).
[10] D.A. Gajewski, R. Chau, and M.B. Maple, Phys. Rev. B **62**, 5496 (2000).
[11] J. Satooka and A. Ito, J. Phys.: Condens. Matter **10**, L711 (1998).
[12] J. García Soldevilla, J.C. Gómez Sal, J.A. Blanco, J.I. Espeso, and J. Rodríguez Fernández, Phys. Rev. B **61**, 6821 (2000).
[13] R. Mathieu and P. Nordblad, Phys. Rev. B **63**, 174405 (2001).
[14] J. Burgy, M. Mayr, V. Martin-Mayor, A. Moreo, and E. Dagotto, Phys. Rev. Lett. **87**, 277202 (2001).
[15] J.M. de Teresa, C. Ritter, M.R. Ibarra, P.A. Algarabel, J.L. García Muñoz, J. Blasco, J. García, and C. Marquina, Phys. Rev. B **56**, 3317 (1997).
[16] S. Süllow, M.B. Maple, D. Tomuta, G.J. Nieuwenhuys, A.A. Menovsky, J.A. Mydosh, and R. Chau, J. Magn. Magn. Mater. **226–230**, 35 (2001).
[17] J.C. Gómez Sal, J.I. Espeso, J. Rodríguez Fernández, N. Marcano, and J.A. Blanco, J. Magn. Magn. Mater. **242–245**, 125 (2002).
[18] T. Yashiro, Y. Hamaguchi, and H. Watanabe, J. Phys. Soc. Jpn. **40**, 63 (1976).
[19] J.C.M. van Dongen, T.T.M. Palstra, A.F.J. Morgownik, J.A. Mydosh, B.M. Geerken, and K.H.J. Buschow, Phys. Rev. B **27**, 1887 (1983).
[20] G. Ehlers, D. Ahlert, C. Ritter, W. Miekeley, and H. Maletta, Europhys. Lett. **37**, 269 (1997).
[21] G. Ehlers, C. Ritter, A. Krutjakow, W. Miekeley, N. Stüßer, Th. Zeiske, and H. Maletta, Phys. Rev. B **59**, 8821 (1999).
[22] I.A. Campbell, J. Phys. F: Met. Phys. **2**, L47 (1972).
[23] A. Hernando, J.M. Rojo, J.C. Gómez Sal, and J.M. Novo, J. Appl. Phys. **79**, 15 (1996).
[24] D. Gignoux, these, L'Université Scientifique et Médicale de Grenoble, 1973.
[25] A. Señas, J. Rodríguez Fernández, and J.C. Gómez Sal, J. Phys.: Condens. Matter **15**, 1339 (2003).
[26] See, for instance, Yu.A. Izyumov, V.E. Naish, and R.P. Ozerov, *Neutron Diffraction of Magnetic Materials* (Consultants Bureau, New York, 1991).
[27] J. Rodríguez-Carvajal, Physica B **192**, 55 (1993). For a more recent version, see Juan Rodríguez-Carvajal, *Recent Developments of the Program FULLPROF*, in Commission on Powder Diffraction (IUCr), Newsletter 26, 12–19 (2001), available at http://journals.iucr.org/iucr-top/comm/cpd/Newsletters/. The program and documentation, as well as the program BASIREPS, can be found at ftp://ftp.cea.fr/pub/llb/divers/.
[28] J.I. Espeso, J. Rodríguez Fernández, J.C. Gómez Sal, and J.A. Blanco, IEEE Trans. Magn. **30**, 1009 (1994).
[29] E.F. Bertaut, Acta Crystallogr., Sect. A: Cryst. Phys., Diffr., Theor. Gen. Crystallogr. **A24**, 217 (1968).
[30] E. Gratz, E. Goremychkin, M. Latroche, G. Hilscher, M. Rotter, H. Müller, A. Lindbaum, H. Michor, V. Paul-Boncour, and M.T. Fernández Díaz, J. Phys.: Condens. Matter **11**, 7893 (1999).
[31] A. Castets, D. Gignoux, and J.C. Gómez Sal, J. Solid State Chem. **31**, 197 (1980).
[32] A. Budziak, H. Figiel, J. Zukrowski, E. Gratz, and B. Ouladdiaf, J. Phys.: Condens. Matter **13**, L871 (2001).
[33] R.J. Elliot, Phys. Rev. **124**, 346 (1961).
[34] J.A. Blanco, J.C. Gómez Sal, J. Rodríguez Fernández, D. Gignoux, D. Schmitt, and J. Rodríguez Carvajal, J. Phys.: Condens. Matter **4**, 8233 (1992).
[35] H.A. Kramers, Proc. R. Acad. Sci. Amsterdam **33**, 959 (1930).
[36] L. Nordström and A. Mavromaras, Europhys. Lett. **49**, 775 (2000).
[37] A. Señas, J. Rodríguez Fernández, J.C. Gómez Sal, and J. Campo, Physica B **350**, e115 (2004).
[38] A. V. Posnikov, V. P. Antropov, and O. Jepsen, J. Phys.: Condens. Matter **4**, 2475 (1992).